Quantum control experiment reveals solvation-induced decoherence

P. van der Walle[a,1], M. T. W. Milder[a], L. Kuipers[a,b], and J. L. Herek[a,b,1]

[a]Stichting voor Fundamenteel Onderzoek der Materie Institute for Atomic and Molecular Physics, Kruislaan 407, 1098 SJ Amsterdam, The Netherlands; and [b]Optical Sciences Group, MESA+ Institute for NanoTechnology, University of Twente, 7500 AE Enschede, The Netherlands

Edited by Nicholas J. Turro, Columbia University, New York, NY, and approved March 26, 2009 (received for review February 18, 2009)

Coherent control holds the promise of becoming a powerful spectroscopic tool for the study of complex molecular systems. Achieving control requires coherence in the quantum system under study. In the condensed phase, coherence is typically lost rapidly because of fluctuating interactions between the solvated molecule and its surrounding environment. We investigate the degree of attainable control on a dye molecule when the fluctuations of its environment are systematically varied. A single successful learning curve for optimizing stimulated emission from the dye in solution is reapplied for a range of solvents with varying viscosity, revealing a striking trend that is correlated directly with the dephasing time. Our results provide clear evidence that the environment limits the leverage of control on the molecular system. This insight can be used to enhance the yield of control experiments greatly.

coherent control | quantum-control spectroscopy | solvation dynamics

Coherent control has been recognized as a potential spectroscopic tool for the study of complex molecular systems (1). With this technique, a molecular system is selectively guided through a potential energy landscape toward a target quantum state by shaped light fields, often employing a closed-loop learning algorithm (2–9). The central idea is that the pulse shapes corresponding to the highest yield contain spectroscopic information concerning the quantum system, yet often the complexity of these pulses hinders their interpretation. Further, achieving control requires coherence in the quantum system under study. In the condensed phase, coherence is typically lost rapidly because of fluctuating interactions between the solvated molecule and its surrounding environment. In simple molecular systems in the gas phase, coherent control has been used to guide the system into a subspace with enhanced decoherence times (10). For solvated molecules, this approach is infeasible because of the complexity added by the environment. Nonetheless, it has been found surprisingly easy to come up with control fields for a wide range of systems (11), from simple atomic systems to large biomolecules. These control fields exert their influence even when the system is interacting with a fluctuating environment such as a protein or a solvent (8). However, in only a few isolated cases has the goal of deriving fundamental properties of the system and the physical mechanism of control been achieved (3, 4, 7). The complexity of the pulse shape hinders the usefulness of coherent control as a research tool, and more progress needs to be made in understanding the basic mechanisms of control and how these apply to a variety of molecular systems. An important objective is to find "rules of thumb" for coherent control, where a given shaped pulse produces a predictable and universal response. A promising route to the realization of this goal is to study a set of systems in which some parameter is systematically varied (12). In this article, we show how the amount of attainable control on a molecule in solution changes when the fluctuations of its environment are systematically varied. By varying the solvent in which a model quantum system is dissolved, we resolve the impact of the environment on our ability to control the system. Particularly, we study how we can manipulate the yield of stimulated emission from a solvated molecule in a range of solvents, thus elucidating their role in the control.

The influence of the solvent on a solvated molecule is typically observed via a Stokes shift, in which the energy of the emitting state is lowered relative to the absorption band. The origin of this effect is the modified electron distribution of the excited state, which prompts the solvent molecules to reposition. Solvation processes are widely studied by using coumarin dyes (13) because the electronic structure of these dyes undergoes a strong change when excited. Furthermore, in nonpolar solvents the solvation process is more amenable to analysis because the complicating effects of hydrogen bonding and solvent rotation are entirely absent. This simple solvation makes the inertial response of the solvent independent in the first 100-fs time window for control (14). For these two reasons we have used the laser dye coumarin 6 dissolved in a range of nonpolar solvents to study the effect of solvation on coherent control.

In contrast to most coherent control strategies, in this study the molecule is excited in the linear absorption regime. Hence, multiphoton interactions, including trivial control based on high-order spectral interference, can be excluded. In the weak-field limit, the control, if any, will be caused by the nontrivial quantum response of the molecule in an open environment (15). In an earlier study of coherent control of a solvated laser dye in the weak-field limit (16), it was found that the overlap of the laser spectrum with the red side of the absorption band of the dye is a significant parameter in the control. The importance of this overlap already suggests that the solvent plays a significant role in the control mechanism because it allows the excitation field to track the change in transition energy in real time as the solvent rearranges. In this study, in contrast to the previous work, we keep the excitation spectrum constant and only modulate the spectral phase. By keeping the amplitude of the excitation spectrum fixed, we ensure that any control achieved will be caused by coherence. To be able to address the dye in all states during the solvent relaxation, we pump at the red side of the absorption band and overlap the laser spectrum with the emission band of the dye (Fig. 1*A*). The optimizations were performed at a moderate laser fluence (1.5×10^{15} photons per cm^2), but because of the low absorption cross-section at the laser wavelength, this fluence is still within the linear absorption regime of the dye ($\approx$2% of the molecules are excited). Excitation pulses were passed through a pulse shaper that modulates the spectral phase by using a liquid crystal mask. This mask was programmed with phases generated by an evolutionary search algorithm. Each iteration, the algorithm generated 40 pulse shapes to test in the experiment and used the intensity of stimulated emission as feedback in a learning loop. This feedback signal was derived from a transient absorption spectrum probed 1 ns after excitation (Fig. 1*B*). Probing at such a long

Author contributions: P.v.d.W., L.K., and J.L.H. designed research; P.v.d.W. and M.T.W.M. performed research; P.v.d.W. and M.T.W.M. analyzed data; and P.v.d.W. and J.L.H. wrote the paper.

The authors declare no conflict of interest.

This article is a PNAS Direct Submission.

[1]To whom correspondence may be addressed. E-mail: p.v.d.walle@amolf.nl or j.l.herek@tnw.utwente.nl.

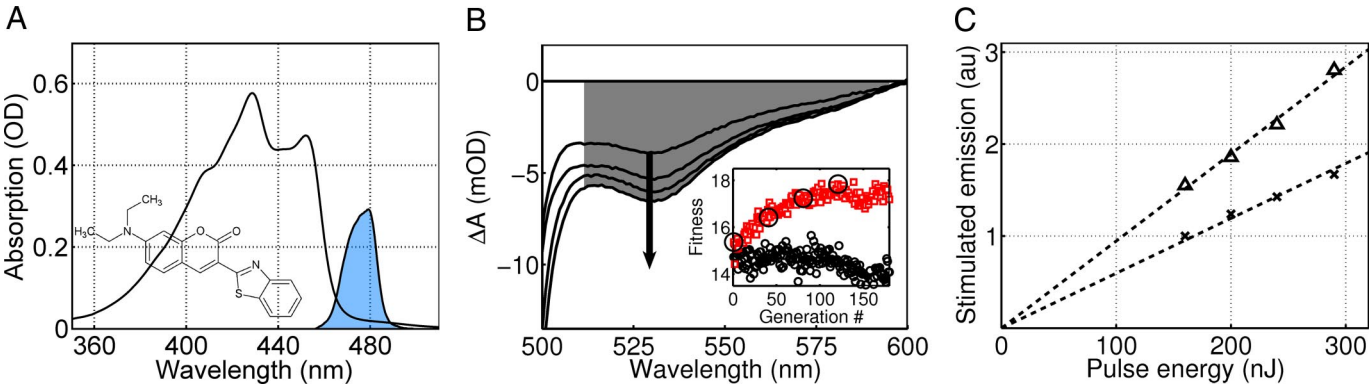

Fig. 1. Details and results of the original open-loop optimization of stimulated emission from Coumarin 6. (*A*) Structure of coumarin 6 and its absorption spectrum in cyclohexane. The laser spectrum (shaded) overlaps with the red wing. (*B*) Pump probe spectrum at 1 ns delay in cyclohexane obtained for four selected generations (circled) of the learning curve (*Inset*). The shaded area indicates the integrated stimulated emission used as a feedback signal for the optimizations. The arrow shows the increase of this area as a result of control. (*C*) Laser energy dependence of the stimulated emission signal for the transform-limited (×) and optimal pulse shape (triangles).

delay ensures full vibrational relaxation of the system and prevents changes in the measured stimulated emission resulting from small shifts of the excitation pulse in time. The search algorithm was aimed to find the pulse shape that maximizes the integrated stimulated emission signal, and it typically converged on a solution in ≈150 generations (red symbols in Fig. 1*B Inset*). Fig. 1*C* shows that the measured stimulated emission depends linearly on the fluence for both the transform-limited and the optimal pulse shapes. This linear dependence indicates that the coherent control is achieved in the weak-field limit.

The best pulse shape in each generation of the optimization was saved. Recording all of the pulse shapes in the optimization procedure allows us to check robustness by remeasuring the optimization curve. Additionally, we can test the generality of the optimization by changing one or more parameters in the experiment (i.e., laser fluence, solvent). The optimization curve can be viewed as the path followed by the algorithm through the "fitness landscape," a multidimensional mountain range of the stimulated emission signal as a function of the separate control parameters. A successful optimization ends at a peak of this mountain range. When the underlying physics have changed, we expect this change to be reflected in the shape of the optimization curve.

Results and Discussion

We ran the optimization on coumarin 6 dissolved in cyclohexane and repeated the measurement by using the recorded pulse shapes with the other solvents. The tested solvents were a range of linear alkanes (hexane, octane, and decane) and their cyclic counterparts. Repeating the pulse shapes rather than reoptimizing for every solvent avoids the possibility of ending up in a different maximum. Consequently, the optimal results can be compared directly and systematically between the systems. The applicability of repeating was checked by a second successful optimization in octane that converged on the same pulse shape and had the same overall yield as the cyclohexane optimization. The remeasured curves were undersampled by only using the pulse shape from every eighth generation. Undersampling shortens the experimental time, reducing the effect of long-term fluctuations in laser power and additionally allows for a longer integration time, resulting in a clearer picture of the shape of the optimization curve. Multiple runs at varying laser intensities were performed to check the power dependence of the optimization result. The ratio of the stimulated emission signals of the transform-limited and optimal pulse was found to be identical at all laser powers, proving that the experiments were carried out in the linear absorption regime.

The fitnesses for the repeated optimizations in the different solvents were normalized to the fitness of the transform-limited pulse (generation 0), allowing for direct comparison (Fig. 2*A*). The order in which the fitnesses corresponding to the pulse shapes were remeasured does not have a clear physical inter-

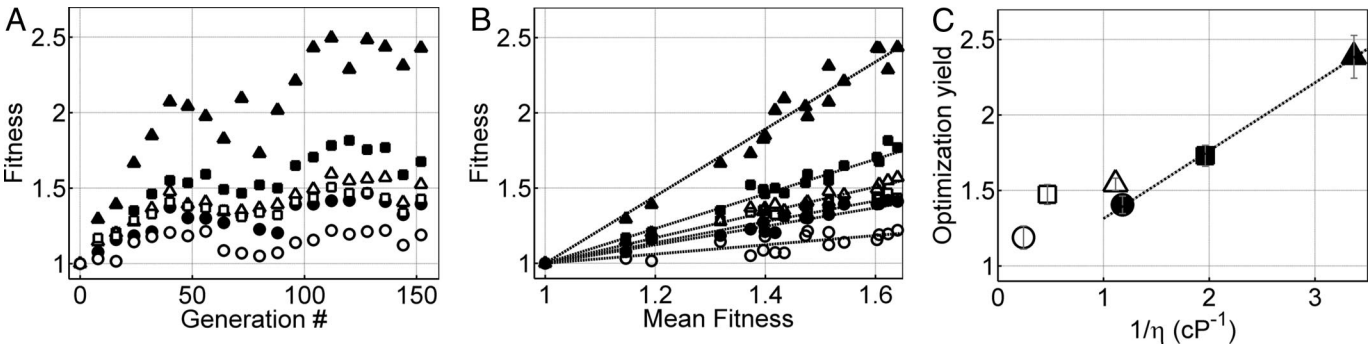

Fig. 2. Solvent dependence of stimulated emission with the pulse shapes from the original optimization. (*A*) Normalized optimization curves for the three linear solvents (filled symbols) hexane (triangles), octane (squares), and decane (circles) and the cyclic solvents (open symbols) cyclohexane (triangles), cyclooctane (squares), and cyclodecane (circles). (*B*) The same fitness values plotted against the average fitness with the corresponding pulse shapes, showing a strong correlation between the solvents. (*C*) The optimization yield relative to the transform-limited pulse versus the inverse solvent viscosity (η). For the linear solvents the optimization yield is inversely proportional to the viscosity. For the cyclic solvents lower-frequency vibrational modes come into play, but a similar dependence is found.

pretation because it depends on the specifics of the search algorithm. Therefore, we plot the normalized fitnesses obtained for each solvent versus the average fitness over all solvents, as measured per pulse shape (Fig. 2*B*). The points sorted in this way now fall on a straight line, revealing a strong correlation between the fitnesses in the different solvents. From this correlation we conclude that the fitness landscapes of the dye in the different solvents are comparable in topology. The slope of the linear fit is an indication of how well the system can be controlled in the corresponding solvent. We call the end point of the linear fits to the data in Fig. 2*B* the optimization yield. The errors on these values were estimated by using a resampling procedure.*

We indeed see that the ability to control the intensity of the stimulated emission depends strongly on the environment. The enhancement of the stimulated emission compared with excitation with the transform-limited pulse varies from 40% in decane to 140% in hexane and from 20% in cyclodecane to 55% in cyclohexane.

The fluorescence quantum yield and lifetime of coumarin 6 is not significantly different in the solvents used. The scaling of the optimization curves is attributed to the different rate at which coherence is lost in the system. Although with coherent control, long-lasting coherences can sometimes be found, we assume for simplicity that those coherences will also depend on solvent fluctuations in the same manner as the electronic dephasing time. Taking this limit of fast fluctuations is a reasonable assumption because a large solvent effect is seen while the optimal pulse is relatively short, suggesting a short dephasing time. A viscoelastic model (17), which captures both the inertial and diffusive response of the solvent, predicts that in this limit of fast fluctuations, the dephasing time is inversely proportional to the solvent viscosity (η) (18). When we plot the optimization yield versus the inverse of the viscosity, we find a linear dependence for the linear solvent molecules (Fig. 2*C*). The cyclic solvents have a different vibrational frequency spectrum, which modifies the dephasing time. This difference means that they are not expected to fall on the same line as the linear solvents, but should nonetheless have a similar dependence on viscosity. The optimization yields indeed show this trend. The viscosity dependence of the optimization yield strongly suggests that decoherence is the fundamental limiting factor in the extent of control.

A representation of the optimal pulse shape is shown in Fig. 3. The pulse is only twice as long as the transform-limited pulse and has a down-chirp, i.e., the blue side of the spectrum arrives before the red side. A potential mechanism associated with a down-chirp is wavepacket localization, in which a linear chirp is matched to the anharmonicity of a vibrational mode (19). However, close inspection of the optimal pulse found here reveals a chirp that is significantly nonlinear, i.e., the chirp rate at the beginning of the pulse (corresponding to a second-order spectral phase of -340 ± 50 fs^2) is much higher than at the end ($-1{,}350 \pm 300$ fs^2). A chirp with such a strong high-order spectral dispersion does not result in an optimally focused wavepacket. An independent optimization, starting from a different random position in the search space, resulted in the same nonlinearly chirped pulse, indicating the importance of this feature for the mechanism of control. Furthermore, we could not achieve the same level of control just by using a linearly chirped pulse.†

The amount of control attained by the shaped pulse is unprecedented at the excitation fluence we used. In large part

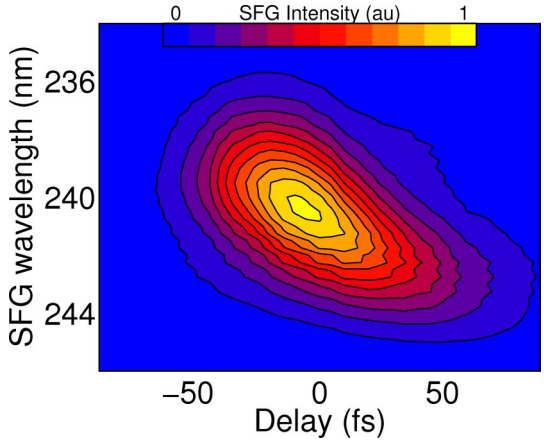

Fig. 3. Two-dimensional representation (X-FROG) of the optimal pulse shape found by the algorithm, showing a nonlinear down-chirp.

the control may be caused by the relatively low fluorescence quantum yield of coumarin 6 in apolar solvents (0.57). This low yield is caused by a loss channel associated with a twisting motion of the amine tail of the molecule (20). A coherent control pathway that avoids this loss channel would thereby maximize population in the excited state, inducing a corresponding increase in the stimulated emission signal.

A nonlinear chirp is typical for a frequency–frequency correlation function, suggesting that the mechanism is tracking the transition frequency. At first sight, such a tracking mechanism may seem counterintuitive for maximizing the population in the excited state; in the high-power limit a pulse with a down-chirp will in general decrease the population transfer through a pump–dump mechanism by tracking the wave packet (6, 21, 22). However, when the laser fluence is reduced, this effect disappears. In the weak-field regime, the down-chirped pulse continues to couple the ground and excited state over the duration of the pulse. By tracking the change in transition energy of the solvated system, the vibrational coherence is transferred from the excited state to the ground state (23). How this effect results in an altered population distribution is at present unclear. The laser field does not interact with the molecule again because this would manifest a nonlinear fluence dependence of the control. At this point we can only speculate that a fast relaxation process in the environment of the molecule is involved. Further experiments and simulations should provide more insight into the exact mechanism of the control, not only in this specific case, but regarding weak-field coherent control in general.

Conclusion

We have found that in the weak-field limit, the optimal excitation pulse for increasing stimulated emission of coumarin 6 in nonpolar solvents features a nonlinear down-chirp. The effect of this pulse shape is contrary to its action in the strong-field regime, where it would be expected to minimize the population in the excited state. More importantly, by systematically varying the solvent we found that the loss of coherence caused by solvent fluctuations, even on the very short time scale of the optimal pulse, is limiting the action of the pulse on the molecule. This generic insight can be regarded as a rule of thumb for control of quantum systems in fluctuating environments. By engineering the fluctuations, for example via a judicious choice of solvent, the yield of control may be varied enormously.

Materials and Methods

The laser system was pumped by a Clark-MXR chirped pulse amplifier (CPA) 2001 (775 nm, 150 fs, 1 mJ, 1 kHz). Part of this light was used to pump a

*The errors on the slopes of the linear fits were determined via bootstrapping by resampling residuals. The error bars in Fig. 2*C* represent the 2σ confidence interval on the end points of the fit, following from this procedure.

†A scan of the chirp from -1500 fs^2 to $+1500$ fs^2 showed a difference of only 4% in the stimulated emission signal.

noncollinear optical parametric amplifier (NOPA) tuned to 475 nm. The NOPA pulses were compressed to 25 fs (transform-limited) using a pulse shaper by optimizing the amount of second harmonic light produced in a beta-barium borate (BBO) crystal. The phase mask needed to obtain the transform-limited pulse was used as a background in further optimizations. For pulse characterization, the Cross-FROG technique was used. The reference pulse was a 25-fs pulse from a second NOPA tuned to 485 nm. The two pulses were mixed in a BBO crystal with a thickness of 25 μm.

The probe was a white light continuum produced by focusing part of the CPA pulses in a sapphire disk. The probe light was recorded with a spectrometer equipped with a home-built diode-array detector. The use of the spectrometer allowed us to separate the stimulated emission signal at its specific wavelength range.

Coumarin 6 was purchased from Exciton and used as received. The solvents were of spectroscopic grade and purchased from Sigma–Aldrich.

The Covariance Matrix Adaptation evolutionary algorithm was used in a (20, 40) strategy with weighted (by fitness value) intermediate recombination. The large number for of individuals that make it into the next generation makes the algorithm more robust to measurement noise. The initial step size was set to 10% of the full range of the parameters.

The phase mask for the pulse shaper was described by the sum of three spline interpolants, a coarse function with 16 parameters and a range of 3 π, a finer function with 64 parameters and a range of 1.5 π, and finally a fine function with 128 parameters and a range of .75 π.

Our experimental procedure is based on a single optimization (cyclohexane as the solvent) of which the best pulse shapes are repeated on all samples. To check the applicability of this procedure, a second optimization was performed on a different sample (octane as the solvent). This optimization resulted in the same pulse shape and the same total amount of control as with the original optimization.

Besides changing the solvent, also the laser fluence was changed, and the fitness curves were remeasured. The response to the transform-limited and the optimal pulse was linear with the fluence in all solvents.

ACKNOWLEDGMENTS. This work is part of the research program of the Stichting voor Fundamenteel Onderzoek der Materie (FOM), which is supported financially by the Nederlandse organisatie voor Wetenschappelijk Onderzoek (NWO). An implementation of the Covariance Matrix Adaptation algorithm was provided by the Leiden Institute of Advanced Computer Science.

1. Rabitz H, De Vivie-Riedle R, Motzkus M, Kompa K (2000) Chemistry: Whither the future of controlling quantum phenomena? *Science* 288:824–828.
2. Judson RS, Rabitz H (1992) Teaching lasers to control molecules. *Phys Rev Let* 68:1500–1503.
3. Daniel C, et al. (2003) Deciphering the reaction dynamics underlying optimal control laser fields. *Science* 299:536–539.
4. Herek JL, Wohlleben W, Cogdell RJ, Zeidler D, Motzkus M (2002) Quantum control of energy flow in light harvesting. *Nature* 417:533–535.
5. Prokhorenko VI, et al. (2006) Coherent control of retinal isomerization in bacteriorhodopsin. *Science* 313:1257–1261.
6. Bardeen CJ, Yakovlev VV, Squier JA, Wilson KR (1998) Quantum control of population transfer in green fluorescent protein by using chirped femtosecond pulses. *J Am Chem Soc* 120:13023–13027.
7. Weinacht TC, Ahn J, Bucksbaum PH (1999) Controlling the shape of a quantum wavefunction. *Nature* 397:233–235.
8. Brixner T, Damrauer NH, Niklaus P, Gerber G (2001) Photoselective adaptive femtosecond quantum control in the liquid phase. *Nature* 414:57–60.
9. Nuernberger P, Vogt G, Brixner T, Gerber G (2007) Femtosecond quantum control of molecular dynamics in the condensed phase. *Phys Chem Chem Phys* 9:2470–2497.
10. Branderhorst MPA, et al. (2008) Coherent control of decoherence. *Science* 320:638–643.
11. Rabitz HA, Hsieh MM, Rosenthal CM (2004) Quantum optimally controlled transition landscapes. *Science* 303:1998–2001.
12. Cardoza D, Baertschy M, Weinacht T (2005) Understanding learning control of molecular fragmentation. *Chem Phys Lett* 411:311–315.
13. Reichardt C (1994) Solvatochromic dyes as solvent polarity indicators. *Chem Rev* 94:2319–2358.
14. Gumy JC, Nicolet O, Vauthey E (1999) Investigation of the solvation dynamics of an organic dye in polar solvents using the femtosecond transient grating technique. *J Phys Chem A* 103:10737–10743.
15. Prokhorenko VI, Nagy AM, Brown LS, Miller RJD (2007) On the mechanism of weak-field coherent control of retinal isomerization in bacteriorhodopsin. *Chem Phys* 341:296–309.
16. Prokhorenko VI, Nagy AM, Miller RJD (2005) Coherent control of the population transfer in complex solvated molecules at weak excitation: An experimental study. *J Chem Phys* 122:184502.
17. Berg M (1998) Viscoelastic continuum model of nonpolar solvation. 1. Implications for multiple time scales in liquid dynamics. *J Phys Chem A* 102:17–30.
18. Berg MA, Rector KD, Fayer MD (2000) Two-pulse echo experiments in the spectral diffusion regime. *J Chem Phys* 113:3233–3242.
19. Lee SH, Jung KH, Sung JH, Hong KH, Nam CH (2002) Adaptive quantum control of DCM fluorescence in the liquid phase. *J Chem Phys* 117:9858–9861.
20. Jones IIG, Jackson WR, Choi C, Bergmark WR (1985) Solvent effects on emission yield and lifetime for coumarin laser dyes: Requirements for a rotatory decay mechanism. *J Phys Chem* 89:294–300.
21. Cao JS, Bardeen CJ, Wilson KR (2000) Molecular π pulses: Population inversion with positively chirped short pulses. *J Chem Phys* 113:1898–1909.
22. Nahmias O, Bismuth O, Shoshana O, Ruhman S (2005) Tracking excited state dynamics with coherent control: Automated limiting of population transfer in LDS750. *J Phys Chem A* 109:8246–8253.
23. Bardeen CJ, Wang Q, Shank CV (1995) Selective excitation of vibrational wave-packet motion using chirped pulses. *Phys Rev Lett* 75:3410–3413.